



AN IMPROVED VERSION OF MODE SHAPE BASED INDICATOR FOR STRUCTURAL DAMAGE IDENTIFICATION

Ho Viet Long, Ho Vinh Ha, Vu Van Toan, Ho Xuan Ba*

Campus in Ho Chi Minh City, University of Transport and Communications, No 450-451 Le Van Viet Street, Ho Chi Minh, Vietnam

ARTICLE INFO

TYPE: Research Article

Received: 20/08/2023

Revised: 12/09/2023

Accepted: 12/09/2023

Published online: 15/09/2023

<https://doi.org/10.47869/tcsj.74.7.3>

* *Corresponding author*

Email: bahx_ph@utc.edu.vn

Abstract. Damage detection is crucial for the operation and maintenance of an existing bridge or building. A vibration-based method is a popular approach that can be used to identify failures based on changes in the dynamic properties. However, this approach often requires information on both healthy and unhealthy states. In this current study, the structural failure determination is carried out through a damage index based solely on the unhealthy state. A combination of the gapped smooth and modal curvature methods is the core of calculating the proposed indicator. In particular, damage scenarios by means of assumed stiffness reduction, and cuts are investigated. Three categories of beam-like structures consisting of a simply supported beam, a cantilever beam, and a free-free beam are used to validate the applicability of the proposed approach. For comparison purposes, the traditional gapped smooth method is implemented. The location of damage can be identified using only displacement mode shapes. Then, damage quantification at the identified location is estimated using a stochastic optimization process. The promising findings indicate that the proposed approach can enhance the effectiveness of damage identification based on vibration data in the unhealthy state of the structures.

Keywords: Gapped smooth method, modal properties, damage identification, AGTO.

@ 2023 University of Transport and Communications

1. INTRODUCTION

Maintaining structural integrity after construction is the primary expectation for every civil engineering structure, such as buildings, bridges, and dams. Throughout their service life, many

unpredictable factors can cause damage to these structures. The accumulation of minor damage can eventually result in severe damage, leading to a shortened lifetime of the structures. The design life and safety of these structures can be ensured if the presence of structural damage can be detected in the early stages of failure. Hence, with an effective structural health monitoring system, failure presence can be exposed before sudden damage happens [1]. Various methods can be used for failure detection, localization, and quantification. One such a method that is of interest to scientists is the vibration-based damage detection method. Based on the dynamic response of the considered structures, the structural safety can be evaluated to make decisions regarding the maintenance activities [2].

The core idea of the vibration-based damage detection method is that the shifts in modal properties can be caused by structural damage. Frequencies, mode shapes, and damping ratios are popular dynamic characteristics that can be used for failure identification. Stiffness reduction or cracks can induce shifts in mode shapes, a drop in frequencies, and an increase in damping ratios [3]. However, the damping ratios are not easy to measure in reality. Therefore, frequencies and mode shapes are more frequently used for damage identification.

Changes in natural frequencies often indicate the presence of damage rather than specifically localizing the damage [4]. Therefore, several authors combined the changes in frequencies with optimization techniques [5], [6], or/and artificial neural networks [7], [8] for damage localization as well as quantification. However, this approach is very time-consuming because it is based on a stochastic optimization process or requires data for network training.

Another approach is to use a damage index derived from frequencies and/or mode shapes, which can directly indicate damage location without an iterative process [9-13]. These studies share the same assumption that information about the pristine and damaged structure is already achieved. However, information regarding intact state is not always available. To address this issue, Ratcliffe developed a 1-D gapped smooth method (GSM) to determine damage based on the damaged state of structures [14]. Yoon then improved this method, to generate a 2D gapped smooth method [15]. Authors in [16] and [17] applied GSM in damage identification of a beam and a plate. These studies demonstrated the effectiveness of the GSM method in diagnosing damage in different structures. With the aim of improving the performance of the approach and advancing its practical application, this study was conducted.

In this current study, damage in three beam-like structures is identified by means of an improved version of the gapped smooth method, namely a curvature-based gapped smooth method. Only unhealthy data of structures are extracted to determine the developed index. The damage location is then accurately identified along the structure where a high peak is detected. Several damage scenarios consisting of assumed stiffness reduction, and cuts are generated in the investigated structures. Results of damage localization using the developed approach and the traditional gapped smooth method are presented to validate the efficiency of the proposed index. Finally, a stochastic optimization procedure is employed to quantify the damage extent regarding frequency changes.

2. METHODOLOGY OF THE PROPOSED APPROACH

2.1 Damage localization

The core idea of the proposed index is derived from the gapped smooth method (GSM). Only displacement mode shapes of the damaged structures are collected to compute the 1-D GSM index for failure localization as follows [14]:

$$gsm_i = \left(\varphi''_{i,d} - C_i\right)_{REAL}^2 + \left(\varphi''_{i,d} - C_i\right)_{IMAGINARY}^2 \quad (1)$$

Where, $\varphi''_{i,d}$ and C_i are curvature and cubic polynomial function at i^{th} point from the unhealthy structure, respectively. The curvature $\varphi''_{i,d}$ is the second derivative of displacement mode shape, which can be identified by central difference approximation:

$$\varphi''_{i,d} = \frac{(\varphi_{i-1,d} - 2\varphi_{i,d} + \varphi_{i+1,d})}{s^2} \quad (2)$$

Where $\varphi_{i,d}$ indicates the displacement mode shape from the unhealthy structure at the i^{th} point and s implies the uniform distance between two successive points.

The second parameter in equation (1), C_i , which is a cubic polynomial function at the i^{th} point, can be interpolated by the following equation [15]:

$$C_i = a_0 + a_1x_i + a_2x_i^2 + a_3x_i^3 \quad (3)$$

Where x_i is the i^{th} position along the investigated structure. Four neighboring curvatures from damaged structure are utilized to identify a_0 , a_1 , a_2 , and a_3 .

Curvature of the gapped smooth index at i^{th} point along the structure is identified as:

$$cgsm_i = \frac{(gsm_{i-1,d} - 2gsm_{i,d} + gsm_{i+1,d})}{s^2} \quad (4)$$

Then, the sudden change in curvature is exaggerated to locate damage position:

$$IGSM_i = \min \left[(cgsm_i, 0)^2 \right] \quad (5)$$

Data from the first five modes should be used to calculate the proposed index:

$$IGSM_k^{normal} = \frac{\sum_{k=1}^{nm} IGSM^{normal}}{nm} \quad (6)$$

Where $IGSM^{normal}$ is an index derived from $IGSM$, which is normalized to a range of [0–1] and nm is number of the considered modes.

2.2 Damage quantification

This section introduces the procedure of damage quantification. Generally, the shift in frequency alone may not be sufficient to identify failure location, but it proves useful in tracking the development of cracks within the structures. Thereby, the cut dimension in the tested

structure is identified solely based on frequency changes. The damage quantification procedure is executed through a stochastic optimization process. Artificial gorilla troops optimizer (AGTO) is employed to control the optimization process. Interested readers may refer to [8] and [18] for more details. This process aims to minimize an objective function derived from the differences in frequencies between the actual and predicted damage states of the observed structures. The value of the objective function is calculated as follows:

$$fitness = \sum_{i=1}^{nm} \left(1 - \frac{f_{predict}}{f_{target}} \right)^2 \tag{7}$$

Where nm is number of the considered modes. $f_{predict}, f_{target}$ indicate the predicted and target frequencies extracted from the FE model.

Figure 1 illustrates the procedure for predicting cut dimensions. In this process, assumed damage consisting of $Lcut(a)$ and $bcut(a)$, is generated in the beam. The first five frequencies of vertical bending modes are collected as a set of target frequencies, denoted as f_{target} . An initial dimension of the cut is randomly generated and input into the FE model, which produces a set of predicted frequencies, denoted as $f_{predict}$. Then the objective function is determined using equation (7). The algorithm AGTO is in charge of optimizing the fitness function until a stop condition is met. When the fitness converges to zero, the predicted state of the structure matches the actual unhealthy one. This implies that the predicted values, $Lcut(p), bcut(p)$ are close to the assumed values, $Lcut(a), bcut(a)$, respectively.

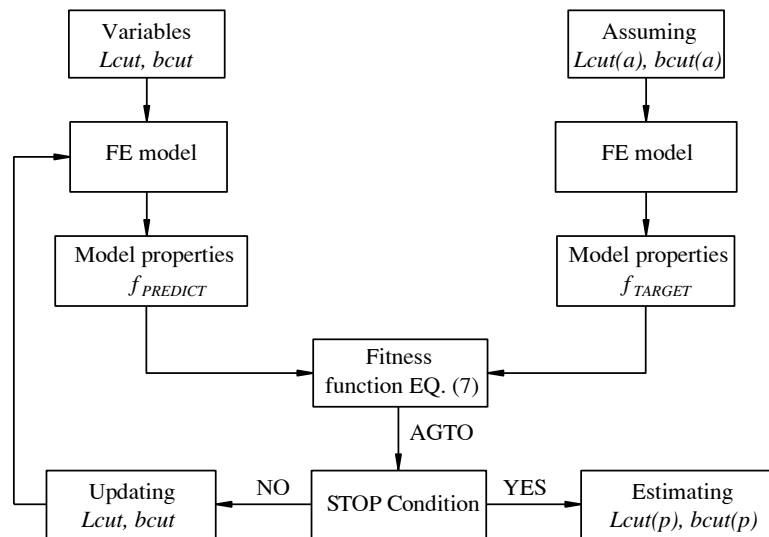


Figure 1. Flowchart of damage quantification using optimization process.

3. CASE STUDY

Three structures, namely a simply supported beam, a cantilever beam, and a free-free beam are considered to verify the efficiency of the proposed index. Assumed stiffness reduction and actual cuts, are used to simulate damages in the tested structures. Each case study includes single and multiple damage scenarios. It should note that damage quantification regarding the cut dimensions is conducted in the third case.

3.1. Simply supported beam-like structure (CS1)

The first case study is a simply supported beam-like structure with a rectangular section. The geometrical dimensions of the beam are $L \times b \times h = 6 \times 0.1 \times 0.2$ (m). L , b , and h are the beam length, width, and height, respectively. The assumed material properties for the beam comprise weight density $\gamma = 7850 \text{ kg/m}^3$, Young's modulus $E = 2 \times 10^5 \text{ MPa}$, and Poisson's ratio $\nu = 0.3$. SHELL181 elements in ANSYS [18] are employed to model the beam with a mesh size of 0.05m.

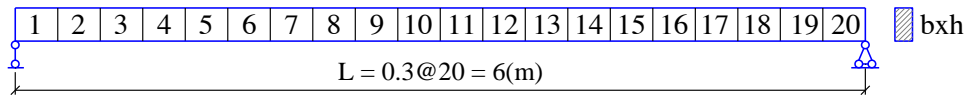


Figure 2. Schematic of the simply supported beam.

In this case study, the beam is composed of 20 segments in Figure 2. Each segment is assumed to be damaged by means of a stiffness reduction factor, β , from 0% to 100%. The stiffness of a segment can be identified as follows:

$$EI_{damage} = EI_{intact} \times (1 - \beta) \tag{8}$$

Where EI implies flexural stiffness of a segment. The beam is healthy if $\beta = 0\%$. In contrast, $\beta \neq 0\%$ indicates unhealthy beam.

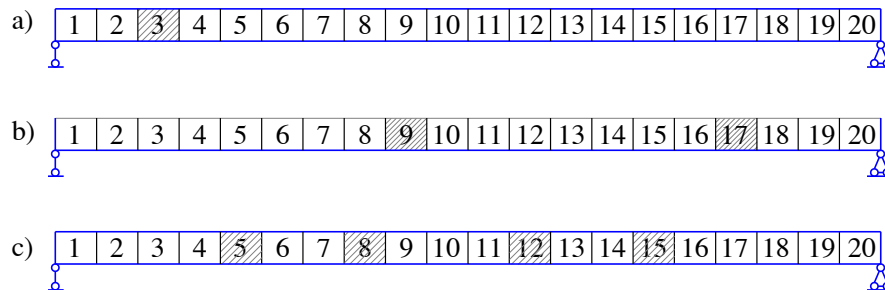


Figure 3. Damage scenarios of CS1.

Three damage scenarios are generated to evaluate the efficiency of the proposed index. Failure localization are indicated using both GSM and IGSM indices. Damaged segments and the corresponding extent are introduced in Figure 3 and Table 1.

To investigate the influence of various modes on the proposed damage localization indicator for Case 1 (single damage), each mode shape is utilized separately to locate the damage. Displacement mode shapes of the first four vertical bending modes are collected for index calculation. The results of damage localization are presented in Figure 4.

Table 1. Elements and stiffness reduction.

Case	Segments				Damage level, β
1	3				7%
2	9		17		40%
3	5	8	12	15	30%

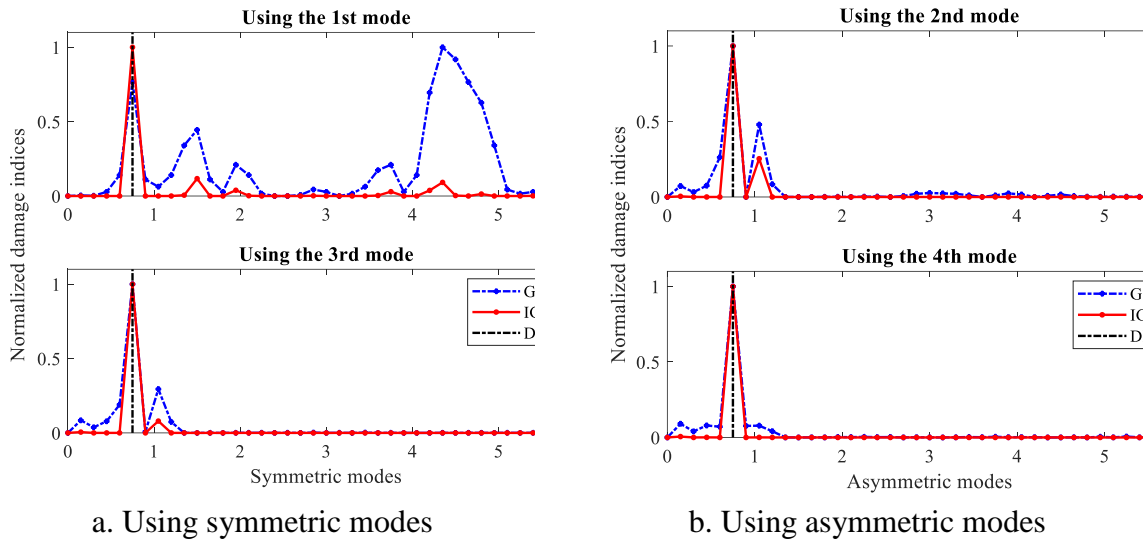


Figure 4. Effects of the first four modes on damage localization (DL1 implies damage location 1).

Generally, higher peaks appear near the damaged region, while smaller peaks may be localized outside the damaged zone. The findings in this case reveal that better results in terms of damage localization can be achieved using higher modes e.g. the 2nd, 3rd, and 4th modes (refers to Figure 4b, c, d). When using only the first mode, a high peak is observed at the damaged segment, but additional peaks are also present in the undamaged zone (see Figure 4a).

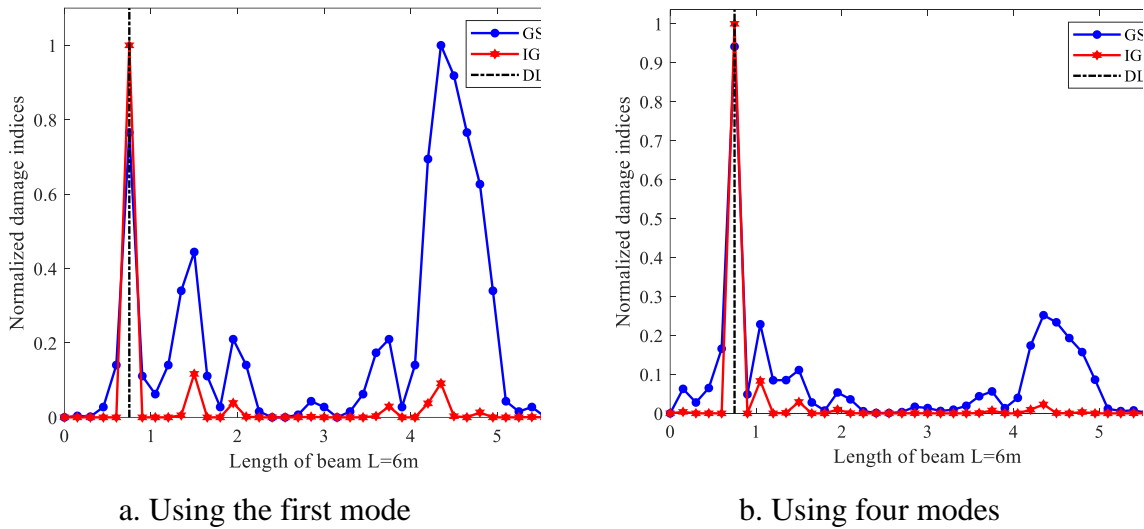


Figure 5. Determination of damage location for case 1 – CS1.

Therefore, to guarantee the quality of damage localization, this study utilizes the first four modes to calculate the proposed indicator. The differences between using 1 and 4 modes are displayed in Figure 5. It illustrates a significant improvement in failure localization when employing four modes compared to using only one mode. By averaging the results from the four modes, the highest peak occurs in the damaged zone, while the other peaks in the undamaged region are notably reduced. Figure 5 also shows that the fault location determination using IGSM outperforms GSM. Even when one or more modes are used, the number of peaks

in the non-damaged region is significantly reduced, further validating the superiority of IGSM in accurate damage localization.

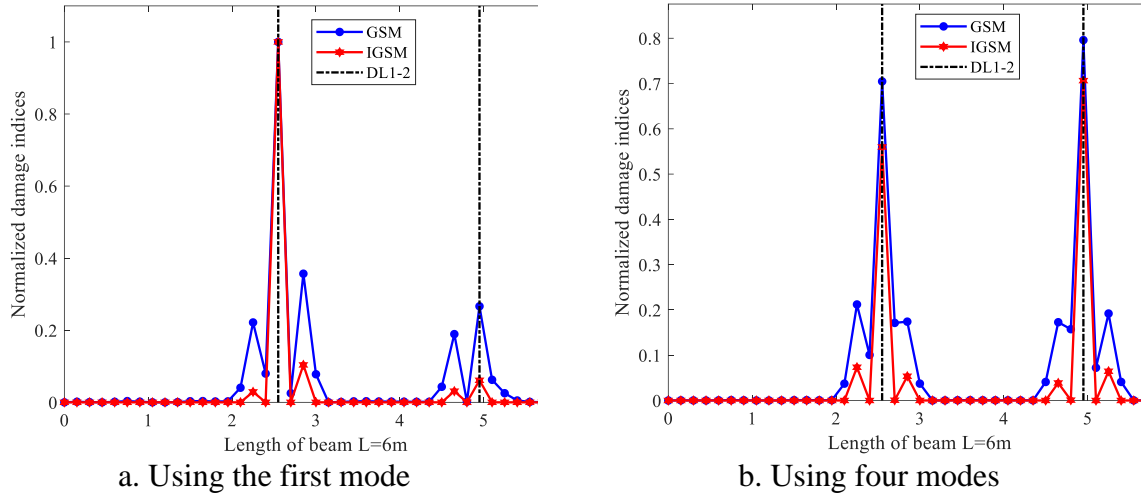


Figure 6. Determination of damage location for case 2 – CS1 (DL2 is damage location 1 and 2).

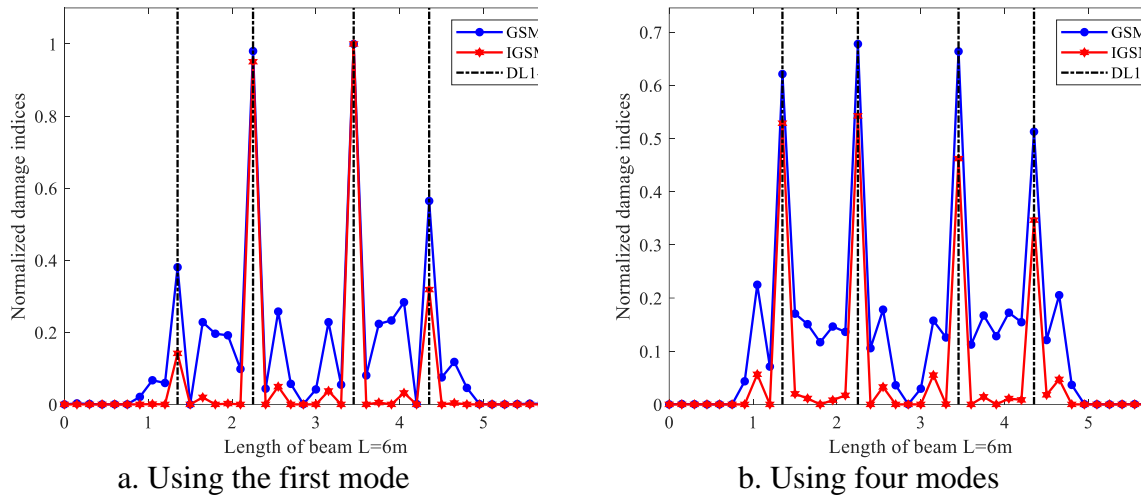


Figure 7. Determination of damage location for case 3 – CS1 (DL1-4 is damage location 1 to 4).

The procedure for multiple damage determination follows the same steps as described above. The first mode and first four modes are used to determine GSM, and IGSM indices. Increasing the number of modes in the index calculation has improved the ability to locate the fault as shown in Figure 6b and Figure 7b. Additionally, the proposed index, IGSM, consistently outperforms the original index, GSM. IGSM exhibits superior performance in localizing the damage to a smaller area compared to GSM (see Figure 6a, b). This distinction becomes more pronounced when increasing the number of failures and reducing the distance between the two failures. In contrast to GSM, IGSM accurately points out clear, high peaks at the fault area, rather than giving warnings at the undamaged site (see Figure 7).

3.2. Cantilever beam-like structure (CS2)

Unlike CS1, the other two cases CS2, and CS3 assess the effectiveness of the proposed method by introducing direct cuts on the beam instead of assuming stiffness reduction. The investigated objective of CS2 is a steel cantilever beam. Geometries and material properties

Transport and Communications Science Journal, Vol. 74, Issue 7 (09/2023), 790-804
 used in the FE model are shown in Figure 8 and Table 2. SHELL181 elements are employed to simulate the beam.

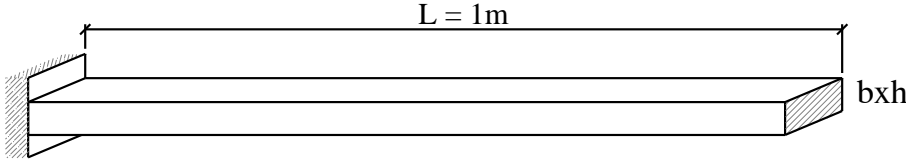


Figure 8. Schematic of the cantilever beam-like structure.

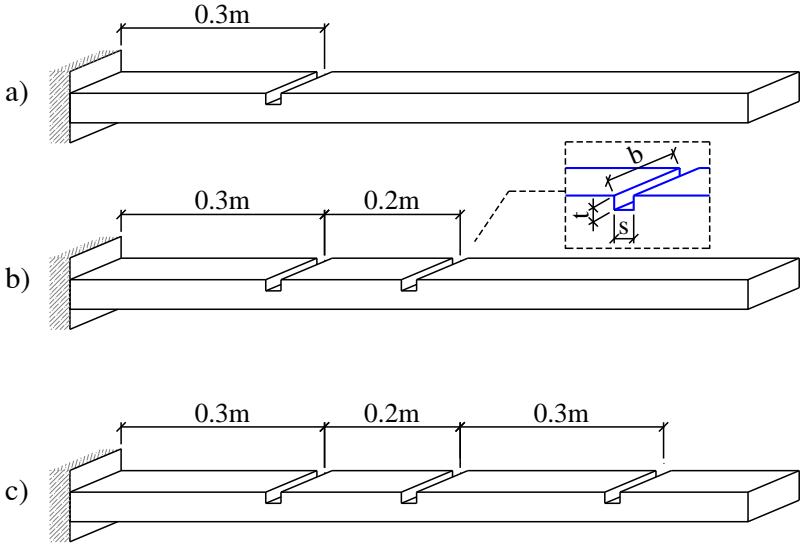


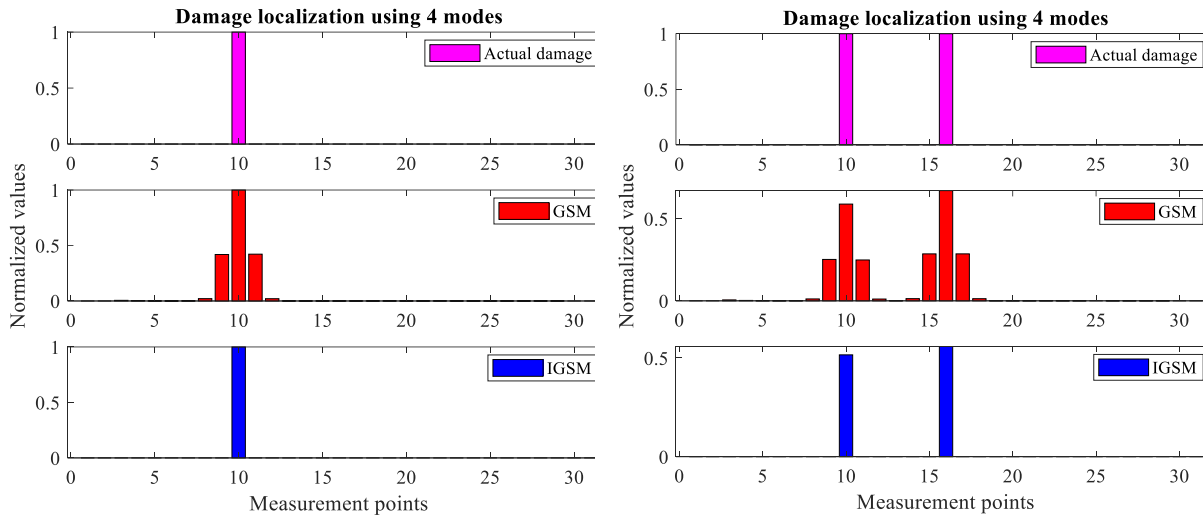
Figure 9. Damage scenarios of CS2.

Three damage scenarios with various cuts are introduced in this section (see Figure 9). The cut dimensions, $t \times s \times b$, are $3.5 \times 5 \times 100$ (mm). Block Lanczos method is used for modal analysis. Dynamic properties such as displacement mode shapes of the first four modes are extracted from the FE model of the beam. Results of damage localization are presented in Figure 10.

Table 2. Properties of the cantilever beam.

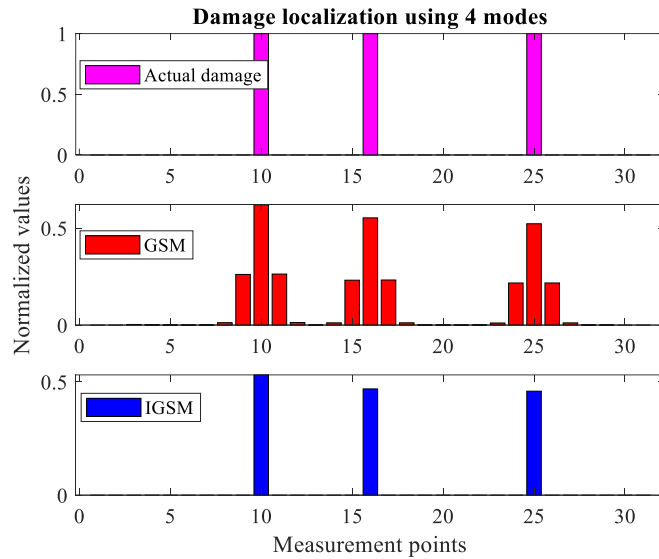
Length $L(m)$	Cross-section $b \times h (m)$	Young's Modulus $E_s (MPa)$	Weight density $\gamma (kg/m^3)$	Poisson's Ratio ν
1	0.1×0.01	2.1×10^5	7850	0.3

Some noteworthy points emerge from the findings. Both GSM and IGSM methods accurately determine the positions of the single cut as well as the multiple cuts in the beam. However, it is evident that the failure warning area when using GSM is relatively wide, encompassing not only the location of the cut but also its vicinity (see Figure 10). Meanwhile, IGSM precisely pinpoints the damaged location coinciding with the position of the cut. This observation confirms that IGSM has a clear advantage over GSM in accurately locating the cut.



a. One cut

b. Two cuts



c. Three cuts

Figure 10. Results of failure localization of CS2.

3.3. Free-free beam-like structure (CS3)

The final case involves a free-free beam that was built based on a measurement caMPaign in a laboratory [20]. Dimensions of the rectangular cross-section of the one-meter-length beam are 70×10(mm). SHELL181 elements are also used to model the beam. Material properties are Young’s modulus $E = 2.1 \times 10^5 \text{ MPa}$, and Poisson’s ratio $\nu = 0.3$. The weight density $\gamma(\text{kg/m}^3)$ is introduced in [20]. Dimensions of the beam are shown in Figure 11.

At various positions along the beam, assumed cuts with same dimensions of 12.5×5×10(mm) are implemented as shown in Figure 12. In CS3, to investigate the effect of two adjacent failures on the ability to locate damage of the proposed indicator, two cuts are

Transport and Communications Science Journal, Vol. 74, Issue 7 (09/2023), 790-804
 spaced 7cm apart (see Figure 12c). Modal properties e.g. frequency and displacement mode shape of the first four vertical bending modes are collected for damage identification.

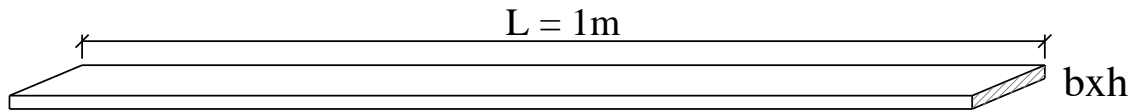


Figure 11. Schematic of the free-free beam-like structure.

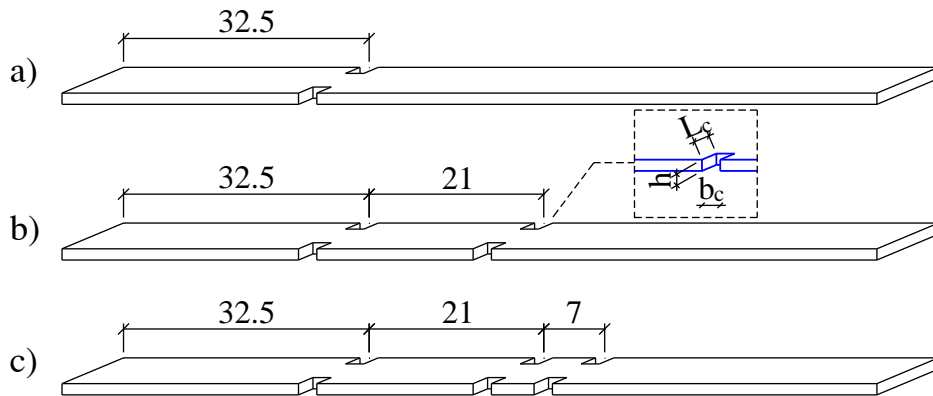


Figure 12. Damage scenarios of CS3 (unit cm).

The damage identification process consists of two steps. In the first step, a damage index is computed using mode shape data. In the second step, cut dimensions regarding length (L_c) and width (b_c) are identified based on the frequencies (see Figure 13b). It is important to note that damage quantification is conducted for case 1, which involves a single cut, as the cut dimensions remain the same for other cases in CS3.

In the damage localization phase, the mode shape data obtained from averaging four modes is utilized to indicate cut locations. Both indices, GSM and IGSM, accurately identify two first cases, single cut, and two cuts. However, when using GSM, some minor peaks are observed at the healthy zone. Figure 13c demonstrates that there is an effect on cut detection when two cuts are placed close to each other. GSM provides a warning about a potential damaged area, but it is not possible to pinpoint the location of the cut. In contrast, IGSM can accurately and clearly locate the cuts. The obtained results confirm the effectiveness of the developed index in failure localization.

In the severity quantification phase, a stochastic optimization process is implemented as discussed in section 2.2. The frequencies obtained from the assumed cut, as presented above, serve as the target frequencies. The optimization process is kicked off with initial values of variables, L_c , and b_c . Some input parameters for AGTO are introduced as follows:

- The investigated objectives are dimensions of the cut regarding to length (L_c) and width (b_c). Consequently, the number of variables under consideration is 2.
- Number of population: 20
- Maximum number of iterations: 25
- Stop condition: The process runs until it reaches the maximum iteration

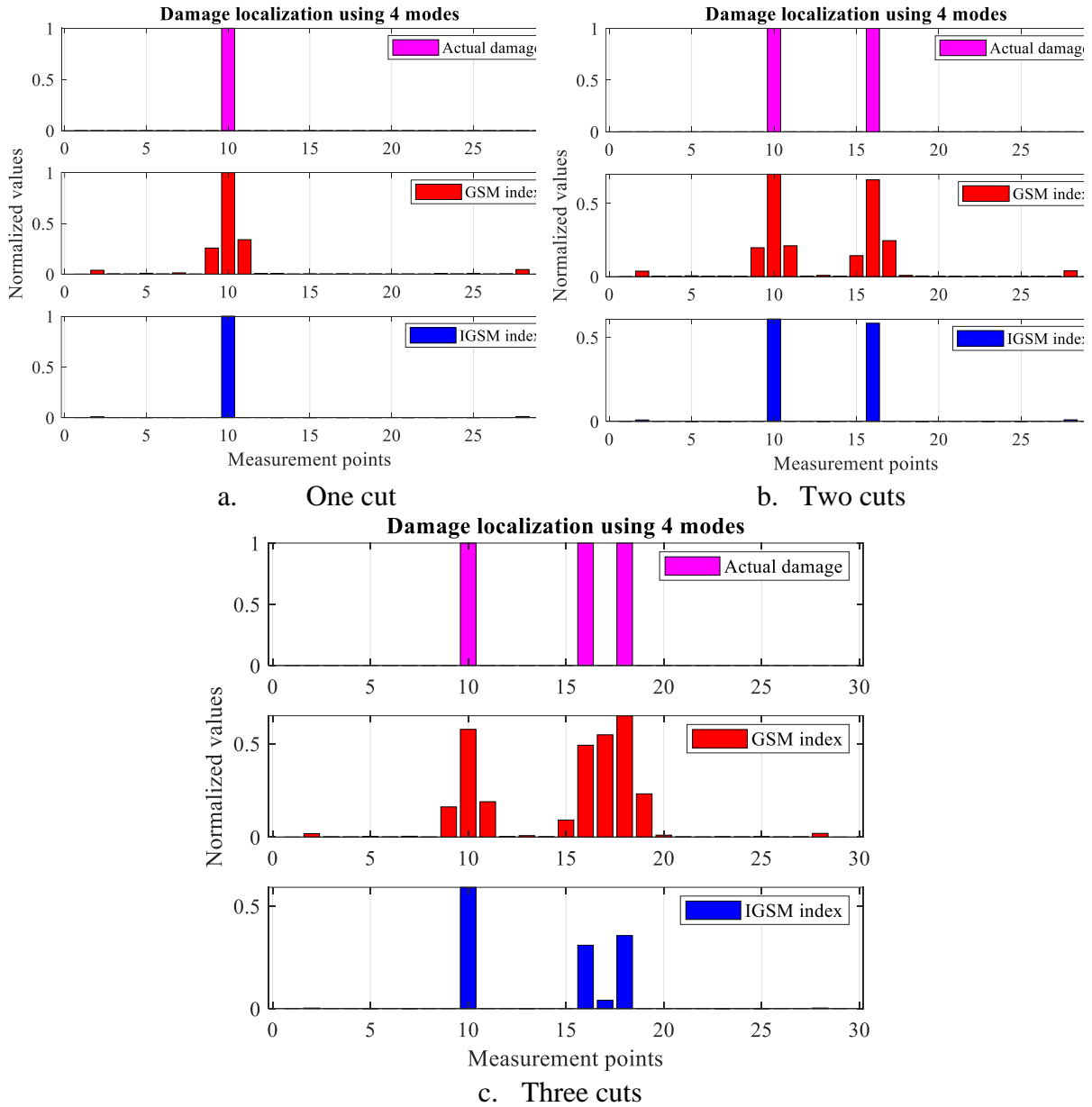


Figure 13. Results of failure localization of CS3.

After 25 iterations, the process is halted, and the convergence of the fitness function is revealed as shown in Figure 14. As the process unfolds, these values are updated iteratively, guided by the objective function computed from equation (7). At the final iteration, the process returns the most suitable set of variables that yields the best fitness i.e. approaching or equaling zero. As a result, severity is identified. The evolutionary process of the two investigated variables is illustrated in Figure 15.

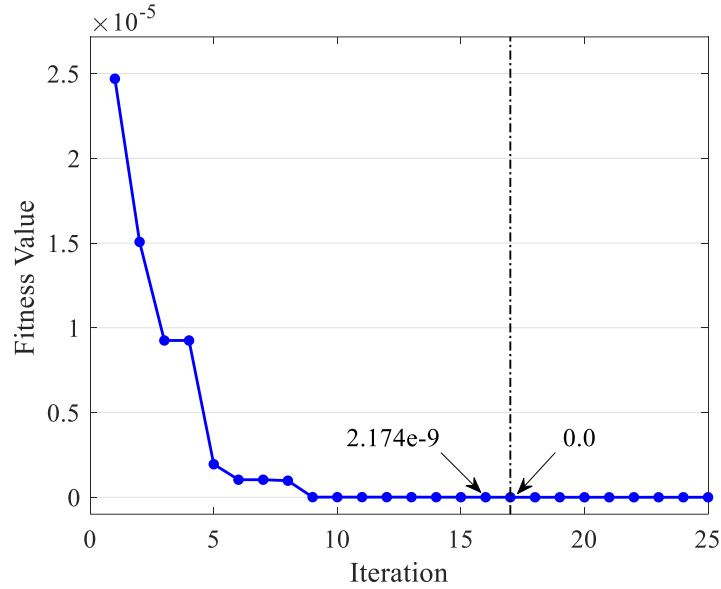


Figure 14. Convergence of the fitness function.

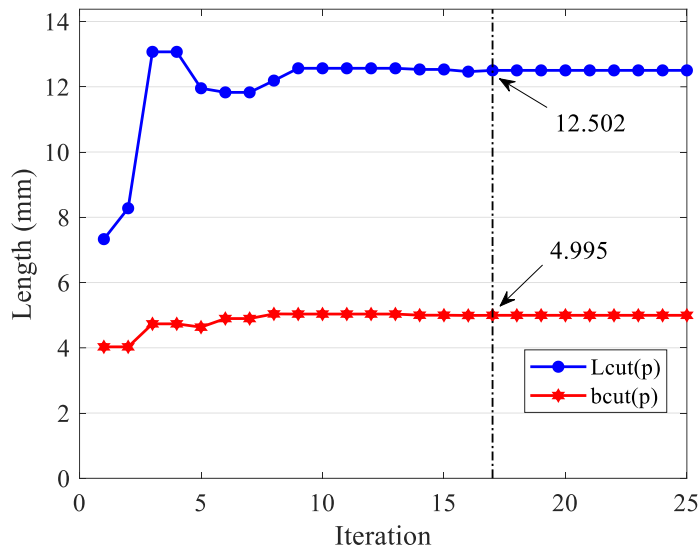


Figure 15. Evolutionary process of damage quantification.

As observed, the fitness function converges to zero during the seventeenth iteration. The optimized values of variables which imply the severity of damage, are 12.502mm and 4.995mm for L_c and b_c , respectively. The comparison between the actual and predicted extents is plotted in Figure 16. The obtained errors are -0.1% and 0.016% for the cut length of 5mm and 12.5mm. Although the noise in the target data has not been considered, the results obtained from the proposed method are very promising. This effect will be considered in future work.

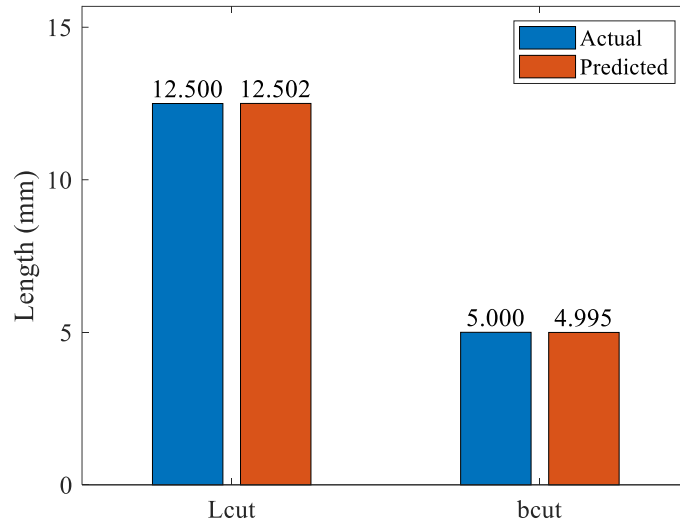


Figure 16. Comparison between actual and predicted dimensions of cut.

4. CONCLUSION

Assessment of structural damage in the absence of intact data is a practical necessity. Many structures, such as bridges, dams, or buildings, have been in service, but the healthy data of these structure are not always available. This lack of data makes it difficult to assess and diagnose structural health condition effectively. Therefore, this study proposed a failure diagnosis solution based on the information of the damaged state of the structure. The findings of the current study confirmed the effectiveness of the proposed method. Some highlights from the study can be pointed out as follows:

- The newly developed index, IGSM has significantly improved the ability to locate defects based on displacement mode shape compared to the traditional GSM index;
- The first mode is well-suited for determining the damage location. However, employing more modes leads to improved failure identification;
- The integration of a stochastic optimization process and frequencies brings superior performance in severity estimation in terms of accuracy, precision, and ease of implementation;

In further study, the damage index should be verified by an experiment. Besides, noise should be considered in damage identification to evaluate the effectiveness of the proposed method.

ACKNOWLEDGMENT

This research is funded by University of Transport and Communications under grant number T2023-PHII-007TD.

REFERENCES

- [1].R. Hou, Y. Xia, Review on the new development of vibration-based damage identification for civil engineering structures: 2010–2019, Journal of Sound and Vibration, 491 (2021) 115741. [https://doi:10.1016/j.jsv.2020.115741](https://doi.org/10.1016/j.jsv.2020.115741)

- [2]. O. Avci, O. Abdeljaber, S. Kiranyaz, M. Hussein, M. Gabbouj, D. J. Inman, A review of vibration-based damage detection in civil structures: From traditional methods to Machine Learning and Deep Learning applications, *Mechanical Systems and Signal Processing*, 147 (2021) 107077. [https://doi: 10.1016/j.ymssp.2020.107077](https://doi.org/10.1016/j.ymssp.2020.107077)
- [3]. M. M. Abdel Wahab, G. De Roeck, Damage detection in bridges using modal curvatures: application to a real damage scenario, *Journal of Sound and Vibration*, 226 (1999) 217–235. [https://doi: 10.1006/jsvi.1999.2295](https://doi.org/10.1006/jsvi.1999.2295)
- [4]. Y. Yang, Y. Zhang, X. Tan, Review on Vibration-Based Structural Health Monitoring Techniques and Technical Codes, *Symmetry*, 13 (2021) 1998. [https://doi: 10.3390/sym13111998](https://doi.org/10.3390/sym13111998)
- [5]. A. Khatir et al., A new hybrid PSO-YUKI for double cracks identification in CFRP cantilever beam, *Composite Structures*, 311 (2023) 116803. [https://doi: 10.1016/j.compstruct.2023.116803](https://doi.org/10.1016/j.compstruct.2023.116803)
- [6]. L. Ngoc-Nguyen et al., Damage assessment of suspension footbridge using vibration measurement data combined with a hybrid bee-genetic algorithm, *Sci Rep*, 12 (2022) 20143. [https://doi: 10.1038/s41598-022-24445-6](https://doi.org/10.1038/s41598-022-24445-6)
- [7]. H. Tran-Ngoc et al., Damage assessment in structures using artificial neural network working and a hybrid stochastic optimization, *Sci Rep*, 12 (2022) 4958. [https://doi: 10.1038/s41598-022-09126-8](https://doi.org/10.1038/s41598-022-09126-8)
- [8]. L. V. Ho, T. Bui-Tien, M. Abdel Wahab, Application of Gorilla Troops' Social Intelligence in Damage Detection for a Girder Bridge, in *Proceedings of the 5th International Conference on Numerical Modelling in Engineering*, M. Abdel Wahab, Ed., Singapore: Springer Nature Singapore, (2023) 11–30. [https://doi: 10.1007/978-981-19-8429-7_2](https://doi.org/10.1007/978-981-19-8429-7_2)
- [9]. L. V. Ho, T. T. Trinh, G. De Roeck, T. Bui-Tien, L. Nguyen-Ngoc, M. Abdel Wahab, An efficient stochastic-based coupled model for damage identification in plate structures, *Engineering Failure Analysis*, 131 (2022) 105866. [https://doi: 10.1016/j.engfailanal.2021.105866](https://doi.org/10.1016/j.engfailanal.2021.105866)
- [10]. A. K. Pandey, M. Biswas, M. M. Samman, Damage detection from changes in curvature mode shapes, *Journal of Sound and Vibration*, 145 (1991) 321–332. [https://doi: 10.1016/0022-460X\(91\)90595-B](https://doi.org/10.1016/0022-460X(91)90595-B)
- [11]. S. Khatir, S. Tiachacht, C. Le Thanh, H. Tran-Ngoc, S. Mirjalili, M. Abdel Wahab, A new robust flexibility index for structural damage identification and quantification, *Engineering Failure Analysis*, 129 (2021) 105714. [https://doi: 10.1016/j.engfailanal.2021.105714](https://doi.org/10.1016/j.engfailanal.2021.105714)
- [12]. L. V. Ho et al., A hybrid computational intelligence approach for structural damage detection using marine predator algorithm and feedforward neural networks, *Computers & Structures*, 252 (2021) 106568. [https://doi: 10.1016/j.compstruc.2021.106568](https://doi.org/10.1016/j.compstruc.2021.106568)
- [13]. L. V. Ho, D. H. Nguyen, G. de Roeck, T. Bui-Tien, M. A. Wahab, Damage detection in steel plates using feed-forward neural network coupled with hybrid particle swarm optimization and gravitational search algorithm, *J. Zhejiang Univ. Sci. A*, 22 (2021) 467–480. [https://doi: 10.1631/jzus.A2000316](https://doi.org/10.1631/jzus.A2000316)
- [14]. C. P. Ratcliffe, Damage detection using a modified laplacian operator on mode shape data, *Journal of Sound and Vibration*, 204 (1997). [https://doi: 10.1006/jsvi.1997.0961](https://doi.org/10.1006/jsvi.1997.0961)
- [15]. M. K. Yoon, D. Heider, J. W. Gillespie, C. P. Ratcliffe, R. M. Crane, Local damage detection using the two-dimensional gapped smoothing method, *Journal of Sound and Vibration*, 279 (2005) 119–139. [https://doi: 10.1016/j.jsv.2003.10.058](https://doi.org/10.1016/j.jsv.2003.10.058)

- [16]. D. H. Nguyen, Q. B. Nguyen, T. Bui-Tien, G. De Roeck, M. Abdel Wahab, Damage detection in girder bridges using modal curvatures gapped smoothing method and Convolutional Neural Network: Application to Bo Nghi bridge, *Theoretical and Applied Fracture Mechanics*, 109 (2020) 102728. <https://doi: 10.1016/j.tafmec.2020.102728>
- [17]. D. H. Nguyen, M. Abdel Wahab, Damage detection in slab structures based on two-dimensional curvature mode shape method and Faster R-CNN, *Advances in Engineering Software*, 176 (2023) 103371. <https://doi: 10.1016/j.advengsoft.2022.103371>
- [18]. B. Abdollahzadeh, F. S. Gharehchopogh, S. Mirjalili, Artificial gorilla troops optimizer: A new nature-inspired metaheuristic algorithm for global optimization problems, *Int J Intell Syst*, 36 (2021) 5887–5958. <https://doi: 10.1002/int.22535>
- [19]. ANSYS, Inc. Southpointe, 275 Technology Drive, Canonsburg, PA 15317, Release 17.2, 2016
- [20]. L. Ho Viet, T. Trinh Thi, B. Ho Xuan, Swarm intelligence-based technique to enhance performance of ANN in structural damage detection, 73 (2022) 1–15. <https://doi: 10.47869/tcsj.73.1.1>